Carbohydrate Polymers 80 (2010) 115–122

Contents lists available at ScienceDirect

Carbohydrate Polymers

journal homepage: www.elsevier.com/locate/carbpol

Binding interaction between aloe polysaccharide and alizarin red by spectrophotometry and its analytical application

Wenxiu Gu [a,*], Hongyan Song [a], Xiaonan Wen [a], Yingying Wang [a], Wenshui Xia [b], Yun Fang [a]

[a] School of Chemical & Material Engineering, Jiangnan University, Wuxi 214122, China
[b] School of Food Science, Jiangnan University, Wuxi 214122, China

ARTICLE INFO

Article history:
Received 18 August 2009
Received in revised form 19 October 2009
Accepted 29 October 2009
Available online 3 November 2009

Keywords:
Alizarin red
Aloe polysaccharide
Spectrophotometry

ABSTRACT

In order to aid the detection of and to reveal the physiological function of aloe polysaccharide (APS), spectroscopic studies of aloe polysaccharide and alizarin red (AR) interaction are presented in this work. APS was identified as an acetylated mannan, which consists of a polydispersed β-1,4-linked mannan substituted with *O*-acetyl groups. The binding interaction between APS and AR was investigated by experiments and theoretical calculation, respectively. The experimental value is in good agreement with the theoretical one. The results show that co-action of the electrostatic and hydrophobic interactions between AR and APS contributes to APS–AR complex chromogenic reaction. Based on this interaction, a new method for spectrophotometric determination of APS with AR is proposed. The maximum absorbances of the complex are at 325 nm and 516 nm. The corresponding linear equations are $A = 0.0109\rho + 0.0441$, $R^2 = 0.9992$ and $A = 0.0121\rho + 0.0288$, $R^2 = 0.9988$. The linear range is 0–60.00 μg/mL and the average recovery is 100.2 ± 5%, RSD ⩽5%.

1. Introduction

Aloe vera L., belonging to the liliaceae family, has been used medicinally for thousands of years owing to possessing curative or healing qualities (Davis, Donato, Hartman, & Haas, 1994; Visuthikosol, Chowchuen, Sukwanarat, Sriurairatana, & Boonpucknavig, 1995). Aloe extract contains many compounds. Of them, aloe polysaccharide (APS) is thought to be the most important component in the gel. It is APS that is responsible for aloe's antiinflammation and immunomodulating activities (Choi et al., 2001; Inan, Sen, Koca, Ergin, & Dener, 2007). Thus, APS has gradually attracted great scientific interest.

The major polysaccharide of aloe gel was reported as an acetylated mannan, which consists of a polydispersed β-1,4-linked mannan substituted with *O*-acetyl groups (Femenia, Sánchez, Simal, & Rosselló, 1999; Mandal & Das, 1980; Manna & McAnalley, 1993; McAnalley, 1988; 1989; McAnalley, Carpenter, & McDaniel, 1994; t'Hart et al., 1989). However, there is a considerable discrepancy in the literature with respect to the structure of the polysaccharide (Tai-Nin Chow, Williamson, Yates, & Goux, 2005). Gowda, Neelisiddaiah, and Anjaneyalu (1979), the first workers to isolate a product by the alcohol precipitation method, found a polysaccharide with a glucose:mannose ratio of 1:19 and a degree of acetylation of 0.78/residue. Linkage analysis showed the presence of β-1,4-linked glucose and mannose, suggesting a linear mannan structure, where mannose residues are randomly substituted with glucose residues (Mandal & Das, 1980). Later work by others suggests three different structures, all having as a β-1,4-linked glucomannan backbone. In the first, β-1,4-linked galactose branches are 2,6-linked to the glucomannan backbone (McAnalley, 1989). In the second, extended galactose branches are α-1,6-linked to the backbone (McAnalley, 1994), and in the third, extended β-1,4-linked mannans are 1,6-linked to the glucomannan backbone (Mandal & Das, 1980). These differences are speculated to arise from the degradation or contamination occurring during processing. In fact, there are many specific steps where polysaccharides can be lost during processing.

The major aloe polysaccharide is important for two reasons. First is the biological activity of the polysaccharide, particularly with regard to the skin. This polysaccharide appears to be an excellent emollient with important moisturizing capability. Furthermore, there are scientific suggestions that the polysaccharide enhances the ability of therapeutic agents to penetrate the skin, thus potentiating their beneficial effect. Second, the level of the polysaccharide is an excellent indicator of the general quality of aloe. An educated consumer will question any product that has been subjected to excessive and harsh processing. Low levels of the polysaccharide indicate an aloe preparation that has been roughly handled. Therefore, it should be readily apparent that good

* Corresponding author. Address: School of Chemical & Material Engineering, Jiangnan University, 1800 Lihu Road, Wuxi 214122, China. Tel.: +86 510 89880770; fax: +86 510 85917763.
E-mail address: guwenxiu@yahoo.com.cn (W. Gu).

0144-8617/$ - see front matter © 2009 Elsevier Ltd. All rights reserved.
doi:10.1016/j.carbpol.2009.10.074

quality aloe products should have the highest possible level of the polysaccharide. The polysaccharide is known as an unstable material. Femenia, Garc a-Pascual, Simal, and Rossell (2003) indicated that heating promoted marked changes in the related functional properties, such as swelling, water retention capacity, and fat adsorption capacity of the bioactive polysaccharide from aloe gel. The influence on the bioactivity and properties of processed products from aloe needs to be considered. Aloe products with too low a content of polysaccharide will show any pharmacological effect.

Therefore, in order to aid the detection of and to uncover the physiological function of APS, spectroscopic studies of APS with spectroscopic probes are strongly advocated. Chen et al. have reported the binding interactions between hyaluronic acid and Azure A (Chen et al., 2005), chondroitin sulfate and methylene blue (Zhou, Jiao, Chen, & Liu, 2002), whereas no systematic investigation on binding interaction between APS and spectroscopic probes has been found in the literature. Alizarin red (AR), which is an anionic dye, has been used for the determination of some inorganic ions and for the interaction mechanism study of protein with small molecules. The molecular structure of AR is shown in Fig. 1a, whereas there is no literature describing AR as a spectroscopic probe for the study of APS. Therefore, the binding interaction between AR and APS was studied by a spectrophotometric method in this work, which is more convenient than usual methods based on physicochemical properties of polysaccarides (Dodgson & Price, 1962; Van Damme, Blackwell, Murphy, & Preston, 1992). According to the theoretical model, the maximum binding number N_C was predicted, which expresses the binding ability of AR with APS. Meanwhile, the experimental value of the maximum binding number N_E, was determined by the spectrophotometric method described in this paper. The research results show that N_E is in good agreement with N_C, which further proves the reliability of the interaction mechanism and the theoretical model between polysaccharides and biological probes.

Moreover, in order to further elucidate the structure–function relationships of the dye–polymer interactions, the polysaccharide (APS) isolated from the extract of the fresh leaf pulp of aloe vera var. chinensis (Haw.) Berg. was identified by size-exclusion HPLC, monosaccharide composition, glycosidic linkage and configuration, IR and elementary analyses. The effects of NaCl and hydroxypropyl-β-cyclodextrin (HP-β-CD) on the chromogenic reaction of APS-AR were studied to gain insight into the nature of the binding interaction.

This study is helpful to explore and recognize the properties, structure, behaviour of APS, and the interaction mechanism with biological probes. Moreover, the study contributes to establish a new simple method for direct determination of APS with AR as a chromogenic reagent.

2. Experimental

2.1. Instruments and reagents

2.1.1. Instruments

A TU-1901 double-beam UV–vis spectrophotometer (Purkinje General, Beijing, China) with 1.0 cm quartz cells was used for measurements of the absorbances and absorption spectra, and pH values were measured with a ZD-2 Automated Titrator (Shanghai 2nd Analytical Instruments Factory, Shanghai, China) which was calibrated with standard buffer solutions of pH 4.01 and 6.86 at 25 °C. All analytical experiments were performed at room temperature. Agilent 6890 GC-5973 MS, Nicolet Magna-Avatar 360, and Vario EL III elemental analyzer were used for structural characterization of APS.

2.1.2. Materials and reagents

Aloe vera var. chinensis (Haw.) Berg., from Yuanjiang County, Yunnan Province, China, was collected and used in this work. AR was purchased from Wenzhou Huaqiao Chemical Reagent Co., Ltd., China. The other reagents were purchased from Shanghai Chemical Company. All the chemicals for the experiments were of analytical grade and freshly distilled deionized water was used throughout. Britton–Robinson and phosphate buffers were used in this work as needed: AR stock solution (1.0000×10^{-3}mol/L, used in the orthogonal experiments, 3.0588×10^{-3}mol/L, used in the molar ratio experiments), APS stock solution (3.927×10^{-7} mol/L, used in the work curves, 5.441×10^{-8}mol/L, used in the molar ratio experiments). Commercial aloe gel raw materials and products were purchased from various processors and marketers in China.

2.1.3. Preparation of aloe polysaccharide standard material

Fresh whole aloe vera var. chinensis (Haw.) Berg. leaves were used as the raw material. Whole leaves were washed with distilled water to remove dirt from the surface. Then, the mucilaginous parenchyma tissue of the aloe leaf was carefully separated from the skin. The filets were extensively washed with distilled water. Fresh aloe filets were homogenized in a blender, and were filtered through eight layers of cheese cloth. The filtrate was adjusted to pH 3.2 with 6 mol/L HCl. Absolute ethanol was added into the gel to achieve gel: ethanol ratio (1:4, v:v). The mixture was stirred for 0.5 h, then laid for 4 h. After separation of the surface suspended matter, the precipitation was separated centrifugally (4000 r/min, 10 min), washed with 80% ethanol, then separated centrifugally

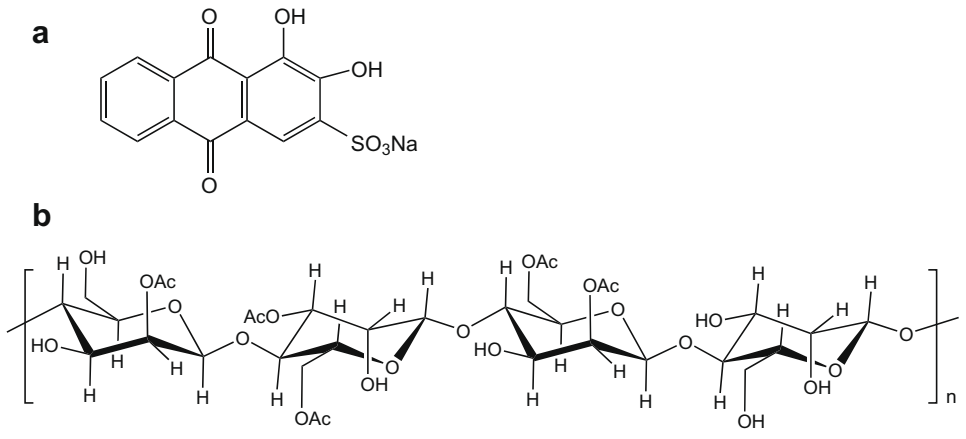

Fig. 1. The structure of alizarin red (a) and aloe polysaccharide (b).

again, washed 3–4 times. The crude product of APS was obtained after the precipitation was lyophilized.

The crude product of APS was dissolved in water again to remove the insoluble residue by passing through a 1.2 μm membrane syringe filter. The filtrate was deproteinized by trichloracetic acid. After repeated processing 2–3 times for thorough deproteinization, the solution was dialysed. After 48 h of continuous dialysis with redistilled water and six changes of water, absolute ethanol was added into the dialysate to reach 80% ethanol for complete precipitation of APS. Subsequently, the precipitation was centrifugally separated, washed 2–3 times with 80% ethanol, then dehydrated with anhydrous diethyl ether. The referential standard product of APS was obtained after the precipitation was lyophilized. The average molecular mass of the APS was determined to be 1100 kDa. The structure of APS was identified by size-exclusion HPLC, monosaccharide composition, glycosidic linkage and configuration, IR and elementary analyses, and is shown in Fig. 1b. The main skeleton of APS is β-(1 → 4)-D linked mannose or glucose with fraction acetylation at C-2, C-3 or C-6.

2.2. Methods

2.2.1. Structural characterization of APS

Purity and molecular mass determinations. Purity and molecular mass of APS employed a size-exclusion HPLC. The following system was used: Waters Linear Ultrahydrogel Column, Waters guard column, and a differential refractometric detector (Shimadzu Corp., Japan). The eluent used was 0.2 mol L^{-1} Na_2Ac in HPLC-grade water, with a flow rate of 0.3 mL min^{-1}. The samples were dissolved in 0.2 mol L^{-1} Na_2Ac and were filtered through a 0.2 μm filter before injection. The molecular mass of APS was estimated by comparison with retention times of high-molecular-mass dextran standards (Sigma).

Monosaccharide composition analysis. Twenty milligrams of APS were hydrolyzed in 2 mL of 2 mol L^{-1} trifluoroacetic acid at 100 °C for 8 h under N_2 atmosphere. The hydrolysis product was evaporated with a stream of N_2, reduced by sodium borohydride and followed by evaporation with a stream of N_2, again. Then, the mixture of pyridine–acetic anhydride (1:1, v/v) was added. After the material was cooled, toluene was added followed by evaporation with a stream of N_2. The monosaccharide composition was analyzed by GC–MS on an Agilent 6890 GC-5973 MS system (Agilent Technologies, Palo Alto, CA, USA).

Enzymatic hydrolysis analysis. Enzymatic hydrolysis of 2 mg mL^{-1} APS solution was done at 40 °C for 40 min with emulsin and maltase, respectively.

Glycosidic linkage and configuration analysis consist of methylation analysis, periodate oxidation and Smith degradation. The polysaccharide was methylated according to the modified Hakomori method (Ciucanu & Kerek, 1984). After methylation complete, the products were hydrolyzed by 2 mol L^{-1} trifluoroacetic acid at 100 °C for 8 h under N_2 atmosphere. The hydrolysis product was evaporated with a stream of N_2, reduced by sodium borohydride. Then, the mixture of pyridine-acetic anhydride (1:1, v/v) was added. After evaporation, partially methylated acetylated monosaccharides were obtained. The analysis was processed by GC–MS after dilution with $CHCl_3$. The procedure for periodate oxidation and Smith degradation was done according to the conventional method. Fifty milligrams of polysaccharide were oxidized with 0.05 mol L^{-1} of sodium metaperiodate at 15 °C in the dark. The periodate-oxidized product was concentrated after the excessive periodate was destroyed by glycol, reduced with sodium borohydride, and then processed by hydrogen type cation exchange resin, eluted by deionized water till the eluate was neutral. Thereafter, hydrolyzation with 2 mol L^{-1} HCl followed by dialysis of the product was performed. The obtained product was analyzed by GC/MS after concentration.

Infrared (IR) and elemental analyses. IR spectrum was measured by a Nicolet Magna-Avatar 360 with KBr disk. Elemental analysis was carried out using a Vario EL III elemental analyzer.

2.2.2. Preparation of the working solutions

APS standard 0.4320 g was weighed on an analytical balance and was dissolved in 1000 mL water to obtain 0.4320 g L^{-1} stock solution. In a series of 10 mL of volumetric flasks, 3.0588×10^{-3} mol L^{-1} AR stock solution 1.00 mL, and APS stock solution 0.05, 0.10, 0.20, 0.40, 0.60, 0.80, 1.00, 1.20, and 1.40 mL were added, respectively. The mixed solutions were diluted to 10 mL with water, then shaken vigorously, laid for 10 min at 25 °C, 1.0 cm quartz cells used for measurements of the absorbances at 516 nm and 325 nm or the absorption spectra in the range of 200–800 nm against reagent blank solution. All the experiments were performed at room temperature.

2.2.3. Preparation of the sample solutions

Samples comprising commercial aloe products, water-soluble gums, non-aloe polysaccharides, etc., were analyzed as received without further purification. About 35 mg of each sample was weighed accurately and was quantitatively transferred into polypropylene conical tubes. Water (20 mL) was added to each sample, and the mixture was placed on an orbital shaker at 200 rpm for 2.5 h, each sample was then filtered through a Whatman 1.25 μm glass microfiber membrane filter. Aliquots (0.40 mL) of each sample were pipetted in triplicate into labeled 10 mL volumetric flasks, and 1.0 mL AR stock solution was added to each flask. The mixed solutions were diluted to 10 mL with water. Absorbance measurements were taken according to the procedure previously described for the standard.

2.2.4. The procedure for the recovery test

Samples of locust gum, guar gum, karaya gum and a commercial aloe capsule were used. Samples were processed according to the procedure introduced in Section 2.2.3. Solutions of the gums and the aloe capsule content at 5 mg/L were spiked with APS standard at concentrations of 20 and 45 mg/L.

2.2.5. The procedures for the identification of binding interaction between APS and AR

In a series of 10 mL of volumetric flasks, AR stock solution 1.00 mL, and APS stock solution 1.00 mL were added successively. Then various amounts of NaCl or 1.0 g/100 mL hydroxypropyl-β-cyclodextrin (HP-β-CD) solution were added, and diluted to 10 mL with water to obtain a series of NaCl test solutions with the concentrations (w/v) of 0.1%, 0.5% and 1% or HP-β-CD test solutions with the concentrations of 0.0, 0.2, 0.4, 0.6, 0.8 and 1.0 g/100 mL. Absorbances were taken according to the procedure previously described for the standard. As to the molar ration experiment, 1.00 mL APS stock solution was transferred into a series of 10 mL volumetric flasks, then 0.1–3.5 mL AR stock solutions were added, respectively. The solutions were diluted with water to 10 mL and were mixed well, the absorption spectra were measured against reagent blank solution.

3. Results and discussion

3.1. The structural characteristics of APS

The yield of APS in this work was 0.35% (w/w) according to the fresh gel. A typical size-exclusion HPLC chromatogram of APS gave only a single and symmetrically sharp peak region:

11.78–17.72 min. The result indicated that APS was homogeneous polysaccharide and did not contain other matters. The estimated equivalent dextran molecular mass of APS was 1100 kDa in reference to the standard dextrans. APS isolated from the extract of the fresh leaf pulp of aloe vera var. chinensis (Haw.) Berg. was identified by size-exclusion HPLC, monosaccharide composition, glycosidic linkage and configuration, IR and elementary analyses. The structure of APS is confirmed and shown in Fig. 1b. APS is a β-(1 → 4)-D linked mannan with fraction acetylation at C-2, C-3 or C-6. The molar ratio of mannose to the acetyl group in the polysaccharide is 1.64:1. GC/MS analysis of the acetylated product shows that APS is composed of mannose, which was further confirmed by IR as the partially acetylated polymannose. Hakomori methylation, periodic acid oxidation and Smith degradation of APS show that it is a straight chain polysaccharide with 1 → 4 linkages. The specific cleavages of the glycosidic bonds by emulsin, but not by maltase, are presented as confirmatory evidence for β-glucosidic linkage in APS, which was further confirmed by IR analysis. The detailed data for APS are as follows: IR(cm^{-1}): 3433 (OH); 2926 (C–H); 1739 (C–O, carbonylic); 1433, 1380 (CH_3); 1250 (C–O–C); 1059 (C–O–C, glycosidic linkage); 898 (β-anomeric configuration); 956, 873 (pyranoid ring) (Synytsya, Čopíková, Matějka, & Machov, 2003; Zhbankov, Andrianov, & Marchewka, 1997). Anal. calcd (%): C, 40.46; H, 6.61; O, 49.36 and N, 0.3. Found for mannose (%): C, 25.00; H, 50.00; and O, 25.00. The peak at 16.50 min in the GC/MS analysis data of alditol acetates from APS shows major fragments at *m/z* (min): 361, 288, 258, 217, 187, 157, 102 and 43, which shows that the component monosaccharide of APS is mannose. GC/MS analysis data of partially methylated alditol acetates from APS: methylated time (1.83 min), the major fragments at *m/z* (min): 43, 87, 101, 117, 128, 160 and 232, 1 → 4 linkage were confirmed due to the generation of 2,3,6-tri-*O*-methymannose. All the retention times were determined with reference to that of 1,5-di-*O*-acetyl-2,3,4,6-tetra-*O*-methylglucitol.

3.2. Absorption spectra of AR at different pH values

AR has two color change pH intervals: 3.7–5.2, 10.0–12.0. The color is yellow in the pH 3.8–5.0 buffer solutions, with only one absorption peak at 422 nm in the range of 350–650 nm. When AR concentration is constant, the absorbance at 422 nm decreases with a bathochromic shift gradually with increasing pH. When pH is higher than 5.4, the color of AR in the buffer solution is red, the absorption peak shifting to 530 nm and the absorbance increasing with the increase of pH. The isobestic point is at 460 nm, as shown in Fig. 2. The result of the absorption spectra is consistent with that of the proton dissociations of AR.

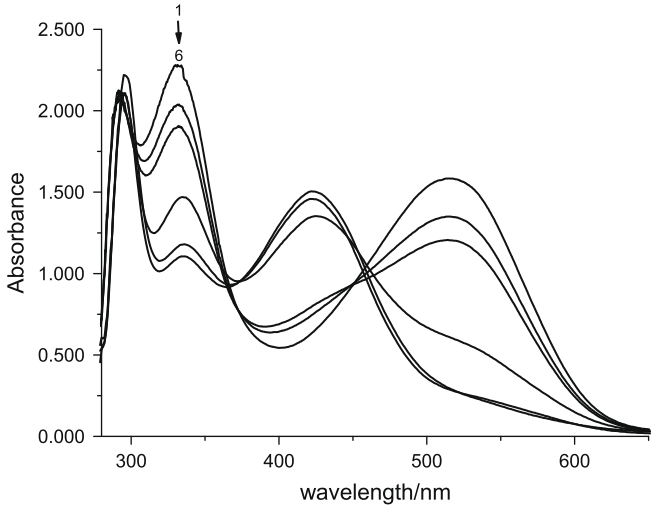

Fig. 2. Absorption spectra of AR in different pH C_{AR}: 3.0588 × 10^{-4}mol/L. Curve Nos. 1–6, the corresponding pHs: 6.6, 6.1, 5.9, 5.2, 4.8, 4.2.

3.3. Optimal chromogenic medium and the maximum absorption wavelength of the complex

It can be inferred from the complex-formation mechanism between AR and proteins by electrostatic interactions that AR is difficult to interact with proteins in near neutral and alkaline conditions (Sun & Jiao, 2002; Zhong, Li, Zhao, & Li, 2004). In addition, taking into account the color change pH intervals of AR 3.7–5.2, 10.0–12.0, the systems whose pH within 5.2–10.0 were chosen primarily to be studied in this work.

The effect of pH on the chromogenic system was studied in a series of Britton–Robinson buffer solutions, the details of pH were as follows: 5.02, 6.09, 6.95, 7.00, 7.96, 8.95, 10.00. The results show that the absorption spectra of AR with APS are almost the same as that of the reagent blank solution in the corresponding pH values. Whereas there exist exactly apparent color differences between the samples and the blank before the buffers are added into the experimental solutions. It was observed in the series of experiments that as long as the buffers were added, the apparent color difference would disappear immediately. Thus a series of phosphate buffers were used as substitutes for Britton–Robinson buffers to find whether the previously adopted ones are suitable. The chosen pH values were as follows: 5.8, 6.0, 6.2, 6.4, 6.8, 7.0, 7.2, 7.4, 7.6, 7.8, and 8.0. The results were the same as that of Britton–Robinson buffers. In view of the result above, the optimal chromogenic medium of APS with AR was confirmed as pure water. The result is shown in Fig. 3. It could be found from Fig. 3 that the

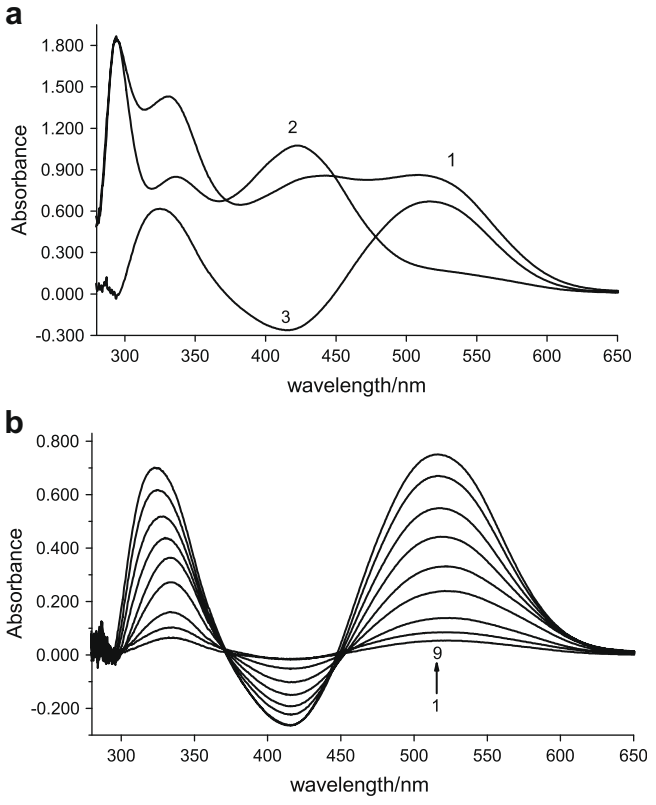

Fig. 3. The chromogenic reaction results of aloe polysaccharide (APS) with alizarin red (AR). (a) Absorption spectra and difference spectrum 1 – AR + APS; 2 – AR; 3 – the difference spectrum of 1 and 2. (b) The series of absorption spectra for the working curves C_{AR}: 3.0588 × 10^{-4}mol/L; In order of the curves: 1–9, C_{APS}/(μg/mL): 2.16; 4.32; 8.64; 17.28; 25.92; 34.56; 43.20; 51.80; 60.48.

second and third absorption peaks of AR under the optimal chromogenic conditions are at λ_2 = 336.5 nm and λ_3 = 422 nm. Once AR bound rapidly with APS at room temperature to form a colored complex, the second peak exhibits a hypsochromic shift and the third peak a bathochromic one. The maximum absorption peaks of the subtractive spectra between AR–APS and AR are at 325 nm and 516 nm. The shift from 422 nm to 516 nm is greater than that of 336.5 nm to 325 nm. Thus, 516 nm was chosen firstly as the work wavelength for the determination of the AR–APS complex. Meanwhile, 325 nm was considered as a subsidiary role.

3.4. Optimal chromogenic conditions, working curves, sensitivity, precision

The effects of the reaction factors on the chromogenic reaction were investigated with a three-factor three-level orthogonal experiment. The details were as follows: the concentration of AR (2.0×10^{-4}, 3.0×10^{-4}, and 4.0×10^{-4} mol/L), chromogenic reaction time (10, 20, and 30 min) and temperature (15, 20, and 25 °C). Anova indicates that the effect order of the factors on the chromogenic reaction is: reaction time > AR concentration > reaction temperature. The corresponding optimal levels: 10 min, 3.0×10^{-4} mol/L and 25 °C.

When the concentration of AR is 3.0588×10^{-4} mol/L, the working curves for APS are $A = 0.0121\rho + 0.0288$, $R^2 = 0.9988$ at 516 nm and $A = 0.0109\rho + 0.0441$, $R^2 = 0.9992$ at 325 nm, respectively, with the linear range of 0–60.00 μg/mL (shown in Fig. 4). The molar absorptivity of the complex was calculated from the slope of the working graph to be 1.3×10^7 L mol^{-1} cm^{-1}. The limit of quantification and the limit of detection for the methods (Long & Wineforder, 1980, 1983) were found to be 1.78 and 0.52 mg L^{-1}, respectively. Ten replicate analyses of a test solution containing 40 μg of APS in 10 mL of solution gave a relative standard deviation of 2.01%.

3.5. The recovery test

The data are shown in Table 1. Aloe polysaccharide recovered was calculated from each experiment, and a recovery mean of 100.2 ± 5% was determined.

3.6. Effect of interfering substances and determination of APS in commercial samples

Common impurities in commercial aloe products are polysaccharides such as malt dextrin, karaya gum, locust gum, guar gum and starch as well as sucrose and glucose. They cannot be distinguished by Fehling test or Dubois test which are the standard determination methods for aloe products. The effects of the common impurities on the determination of APS by the method described above were as follows: Taking into account 0.3456 mg/10 mL APS and the measurement error within ±5%, the amounts of the following substances had no influence on the determination of APS: 1.0458 mg starch, 1.3824 mg glucose and 0.3500 mg malt dextrin, 6.912 mg guar gum, 7.202 mg karaya gum and 8.642 mg locust gum. These results indicate that most common impurities in commercial aloe products can be tolerated in considerable amounts and do not interfere with the determination of APS.

Table 1
Recovery of aloe polysaccharide from spiked samples and non-aloe polysaccharides.

Test solutions	Recovery, %
Guar gum + 20 mg/L APS	99
Locust gum + 20 mg/L APS	98
Karaya gum + 20 mg/LAPS	97
Starch + 20 mg/L APS	98
Malt dextrin + 20 mg/LAPS	101
Gluco se + 20 mg/L APS	99
Commercial aloe capsule I + 20 mg/L APS	98
Commercial aloe capsule II + 20 mg/L APS	99
Guar gum + 45 mg/L APS	101
Locust gum + 45 mg/L APS	101
Karaya gum + 45 mg/LAPS	102
Starch + 45 mg/L APS	103
Malt dextrin + 45 mg/LAPS	103
Gluco se + 45 mg/L APS	101
Commercial aloe capsule I + 45 mg/L APS	102
Commercial aloe capsule II + 45 mg/L APS	101
Mean	100.2 ± 5

3.7. Analytical application

Various aloe samples were collected and processed using the general procedure described in Section 2.2.3. The result is shown in Table 2, which was very precise.

3.8. Intermolecular weak interactions between AR and APS

It could be concluded from Fig. 3 that there exists exactly an interaction between AR and APS. The intensity of the absorption peak at 422 nm declines gradually with increasing APS concentration. Meanwhile, a novel peak emerges and increases gradually at 516 nm. The isobestic wavelength is 447 nm otherwise it will be 460 nm if pH is the only cause for the color change. This indicated

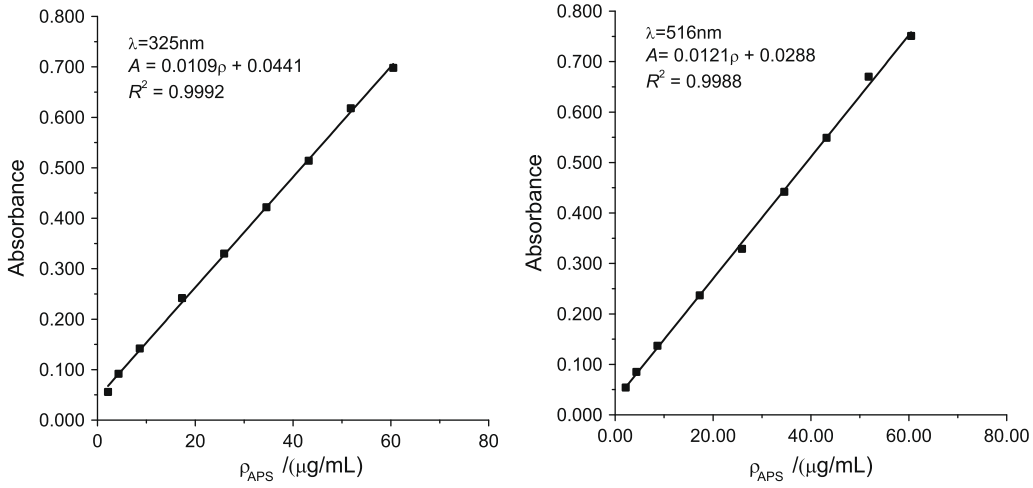

Fig. 4. Working curves of aloe polysaccharide at 325 nm and 516 nm.

Table 2
Determination results of aloe polysaccharide in different samples.

Sample		Fresh aloe gel	100:1 Aloe gel dry powder	200:1 Aloe gel dry powder	Aloe drink I	Aloe drink II	Aloe capsule I	Aloe capsule II
Polysaccharide	λ_1 = 325 nm	0.35	6.79	23.75	0.08	0.09	17.80	18.20
Amount (%)	λ_2 = 516 nm	0.34	6.68	22.69	0.08	0.09	17.82	18.00
RSD (%)		4	5	3	4	3	4	3

that the interaction between AR and APS really exists. There exist many hydroxyl and acetyl groups on APS macromolecular chain, which can form several intramolecular and intermolecular hydrogen bonds in aqueous solutions. It is exactly hydrogen bonds that make APS macromolecular chain a double helix structure with some hydrophobic microregions (Braccini & Perez, 2001; Cheng, Brown & Prud'homme, 2002; Leung, Liu, Koon, & Fung, 2006). Under mild acidic solution, ion-induced dipole attractions between negatively charged AR molecules and neutral APS molecular chains are formed. These weak interactions result in approach of the two molecules to form complexes. Furthermore, the aggregation extent of APS and the numbers of hydrophobic microregion increase simultaneously with increasing APS concentration. Then, the aromatic groups of AR molecules could be attracted into the hydrophobic microregions of APS molecules through hydrophobic interactions. Thus, purplish red AR–APS complex is formed, and a new absorption peak at 516 nm emerges with a gradual increase of the peak intensity. As a result, the color of the solution changes from yellow to purplish red and becomes deeper gradually. Owing to a hypsochromic shift of 13 nm for the isobestic wavelength of APS–AR complex as compared with the absorption maximum of AR, it can be concluded that the binding interaction is not identical with the only protonation of AR in aqueous solutions. The AR–APS purplish red complex is formed by hydrophobic interaction on the foundation of electrostatic interaction between AR and APS.

To further elucidate the characteristics and establish a model of binding interaction between AR and APS, the effect of AR/APS mole ratio on the absorption spectra was studied in this work, the maximum binding number N_E was determined. Meanwhile, the maximum theoretical binding number N_c was calculated from the linear regression equation of interaction theory model. N_E and N_C were compared with each other in this paper, for details see Sections 3.9 and 3.10.

3.9. Effect of AR/APS molar ratio and the maximum binding number N_E

Fig. 5a shows the spectra of the AR–APS complex, which was obtained with constant APS concentration and various AR concentrations. It was concluded from Fig. 5a that the absorbances at 436 nm and 516 nm increase with increasing AR concentration. The new absorption peak at 436 nm does not appear while AR concentration is lower than 2.1×10^{-4}mol/L (sample No. 7), only a peak at 516 nm appears. When AR concentration up to 2.1×10^{-4}mol/L, the peak at 436 nm begins to emerge and the intensity increases with increasing AR concentration. From a structural point of view, the complex can be formed by electrostatic and hydrophobic interaction. But the peak at 436 nm does not appear with a more dilute AR solution. This indicated that the emergence of the peak 436 nm is not only due to electrostatic interaction between AR and APS, but also concerning with the concentration of the combined AR with APS.

To further elucidate the characteristics and establish a model of binding interaction between AR and APS, the effect of AR/APS mole ratio on the absorption spectra was studied, and the maximum binding number N_E was determined as follows. C_D represents AR concentration, and C_P refers to APS concentration. The AR/APS molar ratio may be expressed by the correlation:

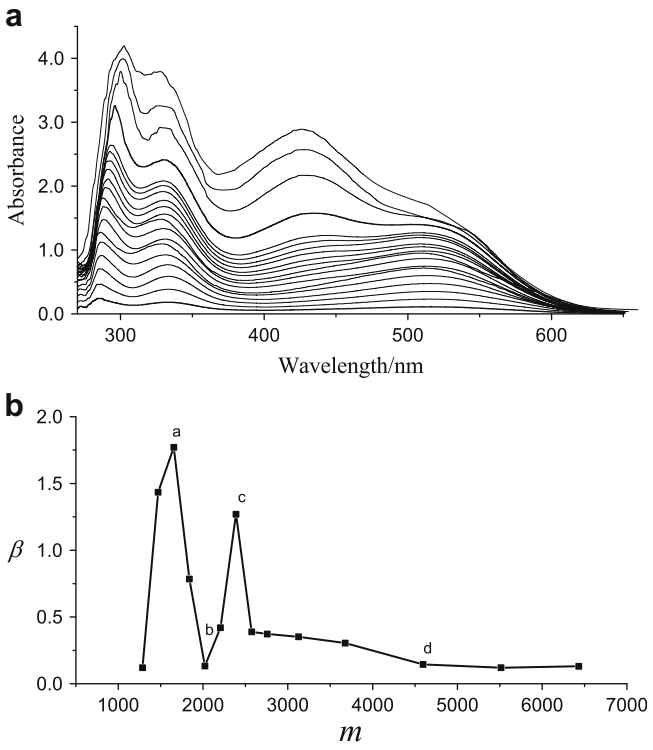

Fig. 5. (a) Absorption spectra of alizarin (AR)–aloe polysaccharide (APS) complexes in different AR concentrations. C_{APS}: 5.441×10^{-8}mol/L, redistilled water medium, in order of the absorption peak at 423 nm from bottom to above: $C_{AR}/10^{-5}$mol/L: 1.0, 2.0, 3.0, 4.0, 5.0, 6.0, 7.0, 8.0, 9.0, 10.0, 11.0, 12.0, 13.0, 14.0, 15.0, 20.0, 25.0, 30.0, 35.0. (b) Relationship between m and β.

$$m = \frac{C_D}{C_P} \quad (1)$$

where A_{422nm} is the absorbance of the test solution at 422 nm, A_{516nm} is the one at 516 nm. ΔA_{422nm} is determined by the subtraction of two neighboring absorbances at 422 nm and ΔA_{516nm} is obtained in the same way. Let

$$\beta = \frac{\Delta A_{516\,nm}}{\Delta A_{422\,nm}} \quad (2)$$

where β is the increase amplitude ratio at 516 nm and 422 nm, the values of β reflect the interaction strength between AR and APS. The larger β is, the stronger the interaction is. The data in Fig. 5a were dealt with relations (1) and (2). The obtained relation between m and β is presented in Fig. 5b.

From Fig. 5b, it was concluded that β begins to increase obviously with the increase of m, and reaches the peak value as m is 1654.1, after that, β decreases gradually with the increase of m, and reaches the wave trough as m is 2021.7, then increases with the rise of m again, reaches the other peak value, then decreases again, and reaches the minimum as m up to 5000.

The experimental phenomena in Fig. 5b can be explained in such a way. Because molecular structure of AR is large, AR molecules can only bind onto the surface of APS molecules through electrostatic ion-induced dipole interaction firstly. Thus, they are

sparsely spread on the long chain of APS molecule according to the principle of minimum energy. At this moment, hydrophobic interaction is too weak to aggregate. Therefore, the new absorption peak at 436 nm is not generated. With m increasing, numbers of binding sites on APS surface decrease gradually, only a few AR molecules can bind onto the surface of APS. Thus, β increases sharply with the rapid increase of m at the beginning, decreases while m reaches a certain value. When m is up to about 2000 (b point), almost all the binding sites on the surface of APS are occupied. If m increases continually, AR molecules begin to bind with the sites inside the molecules of APS. In the same way, the second peak emerges, when m is up to about 4500 (d point), no more AR–APS complex formed again. At this point, the value of m is just the maximum binding number N_E. This indicates that no more interaction between AR and APS takes place any longer. Because no more binding sites on APS are left, m remains constant.

3.10. Calculation of maximum binding number N_c and the binding constant

Jiao and Liu (1998, 1999), Liu, Jiao, Liu, and Chen (2001), Zhou et al. (2002), Gao, Ding, Jiao, Ding, & Chen (2003), Sun, Ding, and Jiao (2006) proposed a mathematical model for the interaction between cationic polysaccharides and anionic biological probes, the corresponding equation for calculating the maximum binding number N_c of spectroscopic probes and polysaccharides is:

$$\Delta A = \Delta\varepsilon(1 + KD_T)/K - \Delta\varepsilon N_C(D_T\Delta\varepsilon/\Delta A - 1)C_P \quad (3)$$

where $\Delta A = A - \varepsilon_F \cdot D_T$, $\Delta\varepsilon = \varepsilon_B - \varepsilon_F$, in which D_T is the total dye concentration in the solution, ε_F and ε_B are the molar absorption coefficients of the free and bound dye, respectively. ε_F and ε_B are constants and are determined from the absorbances of the pure AR solution and the AR–APS solution, respectively. The value of $\Delta\varepsilon$ represents the sensitivity of the dye–polysaccharide-binding assay at a constant dye concentration. C_P is the total polysaccharide concentration in the solution. K is the binding constant, N_C is the maximum binding number. A series of absorbances at 516 nm are shown in Table 3, with a constant AR concentration of 3.0588×10^{-4}mol/L, and various necessary concentrations of APS. The linear regression equation obtained from the data of Table 3 for $(D_T\Delta\varepsilon/\Delta A - 1)C_P$ versus ΔA is:

$$\Delta A = 0.8904 - 0.1482(D_T\Delta\varepsilon/\Delta A - 1)C_P, \quad R^2 = 0.9941$$

The values of K and N_c can be calculated from the intercept and slope of the equation, respectively, $K = 3.218 \times 10^3$, $N_C = 5.17 \times 10^3$. The calculated value of N_C agrees very well with the experimental value of $N_E = 5 \times 10^3$.

3.11. Effect of ionic strength and HP-β-CD on the chromogenic reaction system

The ionic strength was adjusted by different NaCl concentrations, the result is shown in Fig. 6. The absorbance of the complex is rarely affected when NaCl concentration is lower than 0.1%. The absorbances and the slopes of the working curves decrease regularly with increasing NaCl concentration. This indicated that the sensitivity of the probe reaction of the polysaccharide reduced with increasing ionic strength owing to the competition and shielding function of Cl^- and Na^+ on APS and AR. Electrostatic ion-induced dipole interaction may occur between anionic AR and neutral APS according to the molecular structures of them. Therefore, the binding force between AR and APS decreases with respect to the shielding effect of co-existing ions on the charges of AR and induced APS, and the competitive effect of high-concentration anions on the induced positive sites of APS. This indicates that the electrostatic interaction is necessary for the formation of APS–AR complex.

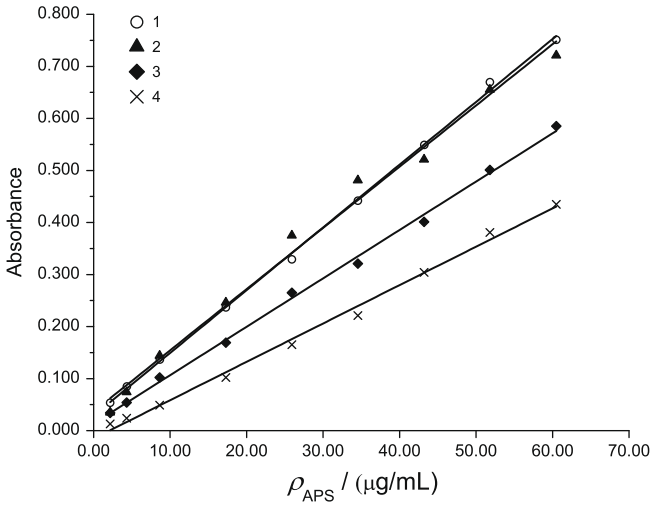

Fig. 6. Effect of ionic strength on the chromogenic reaction of APS-AR at 516 nm 1 – without NaCl, 2 – 0.1% NaCl, 3 – 0.5% NaCl, 4 – 1% NaCl.

Cyclodextrins are cyclic oligosaccharides which have recently been recognized as useful adsorbent matrices. Due to its hydrophobic cavity, cyclodextrins can interact with a wide variety of guest molecules to result in the formation of inclusion complexes (Szente & Szejtli, 2004). These complexes are of interest for scientific research as they exist in an aqueous solution and can be used to study the hydrophobic interactions which are important in the biomedical and environmental fields. The properties of cyclodextrins can be improved by certain chemical modifications, modified cyclodextrins such as hydroxypropyl derivatives are more soluble in water than the unmodified cyclodextrins and their complexes do not precipitate, either. Fig. 7 shows that the absorbance at

Table 3
Data from AR–APS assay in different APS concentrations.

C_P/(mol/L)	ΔA	$(D_T\Delta\varepsilon/\Delta A - 1)C_p$
1.571×10^{-8}	0.237	4.237×10^{-8}
2.356×10^{-8}	0.329	3.920×10^{-8}
3.142×10^{-8}	0.442	3.087×10^{-8}
3.927×10^{-8}	0.549	2.341×10^{-8}
4.709×10^{-8}	0.670	1.450×10^{-8}
5.500×10^{-8}	0.751	0.917×10^{-8}

D_T is the total AR concentration (3.0588×10^{-4}mol/L), C_P is the total APS concentration.

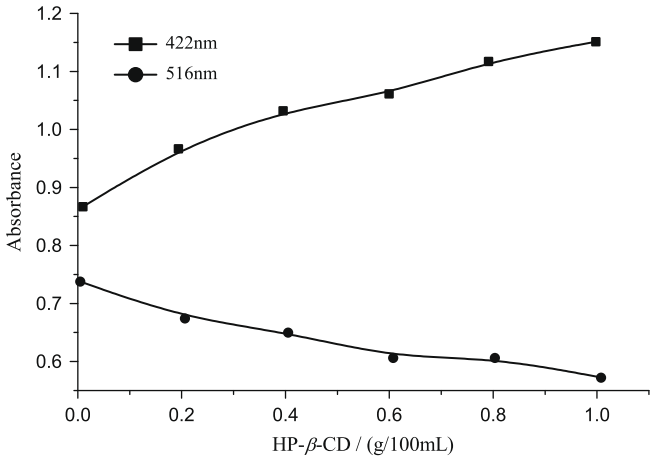

Fig. 7. Effect of HP-β-CD on the chromogenic reaction of APS–AR.

422 nm increases sharply and the absorbance at 516 nm decreases gradually with the increase of HP-β-CD concentration. It can be elucidated that inclusion complexes are formed between HP-β-CD and AR, which destroys hydrophobic interactions between APS and AR. The result shows that the hydrophobic interaction between APS and AR does exist. Thus, it was concluded that the co-action of the electrostatic and hydrophobic interaction between AR and APS contributes to APS–AR chromogenic reaction.

4. Conclusions

APS isolated from the extract of the fresh leaf pulp of aloe vera var. chinensis (Haw.) Berg. was identified by size-exclusion HPLC, monosaccharide composition, glycosidic linkage and configuration, IR and elementary analyses. It was identified as an acetylated mannan, which consists of a polydispersed β-1,4-linked mannan substituted with *O*-acetyl groups at C-2, C-3 or C-6. The molar ratio of mannose to the acetyl group in the polysaccharide is 1.64:1. The binding interaction of APS and AR was studied by a spectrophotometric method. The experimental results show that the co-action of electrostatic ion-induced dipole and hydrophobic interactions between AR and APS contributes to AR–APS complex chromogenic reaction. The aggregation extent of APS macromolecular chain is the essential factor which affects the hydrophobic interaction between AR and APS molecules. The effects of NaCl and HP-β-CD on the chromogenic reaction further confirmed that the electrostatic and hydrophobic interactions between APS and AR do exist. Furthermore, the influence of the molar ratio of AR/APS on the interaction between APS and AR was investigated. The maximum binding numbers were obtained by spectroscopic experiment ($N_E = 5 \times 10^3$) and theoretical model ($N_C = 5.17 \times 10^3$), respectively. The experimental value is in good agreement with the theoretical value.

Based on this interaction, a new method for photometric determination of APS with AR was proposed. The optimal experiment conditions were established. AR can form a colored complex with APS in redistilled water. The maximum absorbances of the complex are at 325 nm and 516 nm. The corresponding linear equations are $A = 0.0109\rho + 0.0441$, $R^2 = 0.9992$ and $A = 0.0121\rho + 0.0288$, $R^2 = 0.9988$. The linear range is 0–60.00 μg/mL and the mean recovery 100.2 ± 5%, RSD ⩽5%. The selectivity and sensitivity of this method are satisfactory and the results are stable.

This APS–AR assay method was considered to be advantageous due to its sensitivity, rapidity and economy. It is useful and convenient for investigation of binding interaction between APS and spectroscopic probes. We hope that the improved mechanistic understanding of such dye–APS complex system obtained from this research will promote more effective use of the assay.

Acknowledgements

This work was financially supported by the Object-oriented Project of State Key Laboratory of Food Science and Technology (No. SKLF-MB-200805) and the Youth Science Foundation of Jiangnan University (No. 104000-52210688).

References

Braccini, I., & Perez, S. (2001). Molecular basis of Ca^{2+}-induced gelation in alginates and pectins: the egg-box model revisited. *Biomacromolecules, 2*(4), 1089–1096.

Chen, Q., Li, X. L., Liu, Q., Jiao, Q. C., Cao, W. G., & Wan, H. (2005). Investigating the binding interaction of azur A with hyaluronic acid via spectrophotometry and its analytical application. *Analytical and Bioanalytical Chemistry, 382*(7), 1513–1519.

Cheng, Y., Brown, K. M., & Prud'homme, R. K. (2002). Characterization and intermolecular interactions of hydroxypropyl guar solutions. *Biomacromolecules, 3*(3), 456–461.

Choi, S. W., Son, B. W., Son, Y. S., Park, Y. I., Lee, S. K., & Chung, M. H. (2001). The wound-healing effect of a glycoprotein fraction isolated from aloe vera. *British Journal of Dermatology, 145*(4), 535–545.

Ciucanu, I., & Kerek, F. (1984). A simple and rapid method for the permethylation of carbohydrates. *Carbohydrate Research, 131*(2), 209–217.

Davis, R. H., Donato, J. J., Hartman, G. M., & Haas, R. C. (1994). Anti-inflammatory and wound healing activity of a growth substance in aloe vera. *Journal of the American Podiatric Medical Association, 84*(2), 77–81.

Dodgson, K. S., & Price, R. G. (1962). A note on the determination of the ester sulphate content of sulphated polysaccharides. *Biochemical Journal, 84*(1), 106.

Femenia, A., Garc a-Pascual, P., Simal, S., & Rossell, C. (2003). Effects of heat treatment and dehydration on bioactive polysaccharide acemannan and cell wall polymers from Aloe barbadensis Miller. *Carbohydrate Polymers, 51*(4), 397–405.

Femenia, A., Sánchez, E. S., Simal, S., & Rosselló, C. (1999). Compositional features of polysaccharides from aloe vera (Aloe barbadensis Miller) plant tissues. *Carbohydrate Polymers, 39*(2), 109–117.

Gowda, D. C., Neelisiddaiah, B., & Anjaneyalu, Y. V. (1979). Structural studies of polysaccharides from aloe vera. *Carbohydrate Research, 72*(1), 201–205.

Gao, G. Z., Ding, L. H., Jiao, Q. C., Ding, Y. L., & Chen, L. (2003). Spectrophotometric determination of chitosan with zincon–chitosan reaction. *Chinese Journal of Analytical Chemistry, 31*(12), 1479–1481.

Inan, A., Sen, M., Koca, C., Ergin, M., & Dener, C. (2007). Effects of aloe vera on colonic anastomoses of rats. *Surgical Practice, 11*(2), 60–65.

Jiao, Q., & Liu, Q. (1998). A mathematical model for interaction of spectroscopic probe with polysaccharides. *Spectroscopy Letters, 31*(7), 1353–1365.

Jiao, Q., & Liu, Q. (1999). Characterization of the interaction between methylene blue and glycosaminoglycans. *Spectrochimica Acta Part A: Molecular and Biomolecular Spectroscopy, 55*(7-8), 1667–1673.

Leung, M. Y. K., Liu, C., Koon, J. C. M., & Fung, K. P. (2006). Polysaccharide biological response modifiers. *Immunology Letters, 105*(2), 101–114.

Liu, Q., Jiao, Q. C., Liu, Z. L., & Chen, H. (2001). The interaction of polysaccharides with a spectroscopic probe: the anion effect on the binding site of heparin. *Spectroscopy Letters, 34*(1), 25–34.

Long, G. L., & Wineforder, D. (1980). Guidelines for data acquisition and data quality evaluation in environmental chemistry. *Analytical Chemistry, 52*(14), 2242–2249.

Long, G. L., & Winefordner, J. D. (1983). Limit of detection. A closer look at the IUPAC definition. *Analytical Chemistry, 55*(7), 712–724.

Mandal, G., & Das, A. (1980). Structure of the glucomannan isolated from the leaves of Aloe barbadensis Miller. *Carbohydrate Research, 87*(5), 249–256.

Manna, S., & McAnalley, B. H. (1993). Determination of the position of the *O*-acetyl group in a β-(1 → 4)-Mannan(acemannan) from Aloe barbardensis Miller. *Carbohydrate Research, 241*, 317–319.

McAnalley, B. H. (1988). Process for preparation of aloe products products, produced thereby and compositions thereof. US Patent Office, Pat. No. 4,851,224.

McAnalley, B. H. (1989). Process for preparation of aloe products. US Patent Office, Pat. No. 4,735,935.

McAnalley, B. H. (1994). Aloe compositions and uses thereof. EP Patent Office, Patent No. 0,382,840.

McAnalley, B. H., Carpenter, R. H., & McDaniel, H. R. (1994). Uses of aloe products. US Patent Office, Pat. No. 5,308,838.

Sun, W., Ding, Y. Q., & Jiao, K. (2006). Voltammetric determination of heparin based on its interaction with brilliant cresyl blue. *Chemical Research in Chinese Universities, 22*(3), 406–409.

Sun, W., & Jiao, K. (2002). Linear sweep voltammetric determination of protein based on its interaction with alizarin red S. *Talanta, 56*(6), 1073–1080.

Synytsya, A., Čopíková, J., Matějka, P., & Machov, V. (2003). Fourier transform Raman and infrared spectroscopy of pectins. *Carbohydrate Polymers, 54*(1), 97–106.

Szente, L., & Szejtli, J. (2004). Cyclodextrins as food ingredients. *Trends in Food Science & Technology, 15*(3–4), 137–142.

Tai-Nin Chow, J., Williamson, D. A., Yates, K. M., & Goux, W. J. (2005). Chemical characterization of the immunomodulating polysaccharide of aloe vera L.. *Carbohydrate Research, 340*(6), 1131–1142.

t'Hart, L. A., Van den Berg, A. J., Kuis, L., Van Dijk, H., & Labadie, R. P. (1989). An anti-complementary polysaccharide with immunological adjuvant activity from the leaf parenchyma gel of aloe vera. *Planta Medica, 55*(6), 509.

Van Damme, M. P. I., Blackwell, S. T., Murphy, W. H., & Preston, B. N. (1992). The measurement of negative charge content in cartilage using a colloid titration technique. *Analytical Biochemistry, 204*(2), 250–257.

Visuthikosol, V., Chowchuen, B., Sukwanarat, Y., Sriurairatana, S., & Boonpucknavig, V. (1995). Effect of aloe vera gel to healing of burn wound a clinical and histologic study. *Journal-Medical Association of Thailand, 78*, 403.

Zhbankov, R. G., Andrianov, V. M., & Marchewka, M. K. (1997). Fourier transform IR and Raman spectroscopy and structure of carbohydrates. *Journal of Molecular Structure, 436*, 637–654.

Zhong, H., Li, N., Zhao, F., & Li, K. (2004). Determination of proteins with alizarin red S by Rayleigh light scattering technique. *Talanta, 62*(1), 37–42.

Zhou, S. G., Jiao, Q. C., Chen, L., & Liu, Q. (2002). Binding interaction between hondroitin sulfate and methylene blue by spectrophotometry. *Spectroscopy Letters, 35*(1), 21–29.